

Measurement report: Vanadium-containing ship exhaust particles detected in and above the marine boundary layer in the remote atmosphere

Maya Abou-Ghanem¹, Daniel M. Murphy¹, Gregory P. Schill¹, Michael J. Lawler^{1,2}, and Karl D. Froyd^{1,2}

5 ¹Chemical Sciences Laboratory, National Oceanic and Atmospheric Administration, Boulder, 80305, USA

²Cooperative Institute for Research in Environmental Sciences, University of Colorado Boulder, Boulder, 80309, USA

Correspondence to: Maya Abou-Ghanem (maya.abou-ghanem@tofwerk.com)

Abstract. Each year, commercial ships emit over 1.67 Tg of particulate matter (PM) pollution into the atmosphere. These ships rely on the combustion of heavy fuel oil, which contains high levels of sulfur, large aromatic organic compounds, and metals. Vanadium is one of the metals most commonly associated with heavy fuel oil and is often used as a tracer for PM from ship exhaust. Previous studies have suggested that vanadium-containing PM has impacts on human health and climate due to its toxicological and cloud formation properties, respectively; however, its distribution in the atmosphere is not fully understood, which limits our ability to quantify the environmental implications of PM emitted by ships. Here, we present data obtained from Particle Analysis by Laser Mass Spectrometry (PALMS) instrument on the NASA DC-8 aircraft during the 2016–2018 Atmospheric Tomography Mission (ATom) and show that ~1% of the accumulation mode particles measured in the marine boundary layer of the central Pacific and Atlantic Ocean contain vanadium. These measurements, which were made without targeting ship plumes, suggest that PM emitted by ships is widespread in the atmosphere. Furthermore, we observed vanadium-containing ship exhaust particles at altitudes up to 13 km, which demonstrates that not all ship exhaust particles are immediately removed via wet deposition processes. In addition, using laboratory calibrations, we determined that most vanadium-containing ship exhaust particles can contain up to a few wt % vanadium. This study furthers our understanding of both the chemical composition and distribution of PM emitted by ships, which will allow us to better constrain the climate, health, and air quality implications of these particle types in the future. We note that these data were collected prior to the 2020 International Maritime Organization (IMO) sulfur regulation and stand as a reference for understanding how ship emissions have evolved in light of these regulations.

1 Introduction

The world economy is highly reliant on the shipping industry, which is responsible for facilitating 80% of global trade (UNCTAD, 2022). The strong demand for the import and export of goods supports approximately 50,000 active ships worldwide (UNCTAD, 2018). Traditionally, these fleets have relied on the combustion of heavy fuel oil for vessel propulsion,

30 which is the residue obtained from petroleum distillation. These low-cost fuels are rich in aromatic hydrocarbons, sulfur, and heavy metals; as a result, emissions from marine vessels have a significant contribution to global air pollution, with estimated emissions of 21 and 12 Tg of NO_x and SO_x, respectively (Eyring et al., 2005). Additionally, the combustion of heavy fuel oil from ships contributes to approximately 1.67 Tg y⁻¹ of particulate matter with an aerodynamic diameter of 10 μm or smaller (PM₁₀) (Eyring et al., 2005). These particulates emitted by ships can mix with marine aerosol and influence the formation of
35 clouds (Hobbs et al., 2000), which can have climate impacts by altering Earth's radiative budget (Lauer et al., 2007). Furthermore, it is estimated that the inhalation of PM emitted from ships contributes to 60,000 human deaths per year (Corbett et al., 2007). One toxic component of this PM is heavy metals, which have been previously linked to cardiovascular damage (Ye et al., 2018) and lung cancer (Bollati et al., 2010).

Many analytical techniques have characterized heavy metals in PM emitted by ships including, inductively coupled plasma
40 mass spectrometry (Moreno et al., 2010; Celo et al., 2015) and X-ray fluorescence (Moldanová et al., 2013); however, these bulk analysis techniques have low temporal and spatial resolution because they require samples to be collected onto filters prior to analysis. To overcome these limitations, single-particle mass spectrometry has been used for real-time chemical analysis of PM from ships. This technique is advantageous because it characterizes both the non-refractory (e.g., organic, nitrate, and sulfate) and refractory (e.g., heavy metals) components of individual particles emitted from ships, which can
45 provide information on particle mixing state (i.e., internally or externally mixed). For example, previous single-particle mass spectrometry studies have classified ship-borne PM as internal mixtures based on unique chemical signatures in the mass spectra, which include vanadium, nickel, iron, organics, nitrate, ammonium, and sulfate (Ault et al., 2010; Passig et al., 2021; Froyd et al., 2019; Healy et al., 2009; Anders et al., 2023).

Over the past several decades, vanadium and nickel have been used as chemical tracers for ship exhaust particles in the marine
50 atmosphere (Viana et al., 2009; Zhang et al., 2014). To our best knowledge, these chemical signatures have only been used for the identification of ship exhaust particles and not for the quantification of heavy metals in single particles. In addition, the majority of single-particle mass spectrometry measurements of PM from ships have been conducted at port or within ship plumes, which limits our ability to understand how the chemical composition of ship PM evolves as it undergoes atmospheric aging.

55 From 2016-2018, global in-situ aircraft-based aerosol measurements were made using the particle analysis by laser mass spectrometry (PALMS) instrument, which was on board the NASA DC-8 aircraft during the Atmospheric Tomography Mission (ATom) (Thompson et al., 2022). Analysis of the comprehensive PALMS datasets obtained during ATom reveal that ~1% of the accumulation mode particles in the marine boundary layer (MBL) resembled that of PM emitted from ships due to the presence of vanadium, nickel, iron, sulfate, and organic material. These measurements, which were made without
60 specifically targeting ship plumes, suggest that PM from ships can remain in the atmosphere for extended periods of time. In this work, we present the application of laboratory calibrations to the ATom data set to quantify vanadium in individual ship particles. In addition, we also investigate how the chemical composition of these particles changes as they are processed in the atmosphere.

The measurements presented in this study are prior to the 2020 International Maritime Organization (IMO) sulfur regulation, which was aimed to reduce the air pollution burden of marine vessels by mandating the use of cleaner fuels. Specifically, this policy required the global shipping industry to transition from 3.5 to 0.5 wt % sulfur fuel (IMO 2020 – cutting sulphur oxide emissions, 2023). Even stricter sulfur regulations (0.1 wt %) have been implemented in emission control areas (ECAs), which have been implemented near certain coastal regions in the US, Canada, Europe, and China to protect populations residing near highly trafficked shipping areas. The sulfur targets in the 2020 IMO regulation and ECAs can be achieved through the addition of scrubbers to capture SO₂ emitted during heavy-fuel oil combustion or by using cleaner fuel alternatives (e.g., distillates or natural gas) (Lehtoranta et al., 2019). These methods can also result in a reduction in the total number of vanadium-containing particles emitted by ships (Yu et al., 2021; Xiong et al., 2023); however, the reductions are not complete as vanadium-containing ship exhaust particles are still detected in ECAs (Passig et al., 2021; Xiong et al., 2023). Although this study was conducted before the 2020 IMO policy, it provides detailed baseline compositional and geographical measurements for vanadium-containing ship exhaust particles in the remote atmosphere that can be used to compare the changes in distribution, chemical composition, and atmospheric aging of this particle type after the enactment of the sulfur policy.

2 Methods

2.1 Single-particle measurements during ATom using PALMS

The ATom dataset is especially valuable for understanding the prevalence of ship particles because the globe-spanning flights were largely predetermined and made no effort to target or avoid ship plumes or shipping lanes. Although this sampling method results in a loss of detail about fresh ship exhaust particles, it provides fairly unbiased measurements for these particles and allows for a widespread assessment of their atmospheric transport, lifetime, and chemical aging processes. Specifically, ATom consisted of over 48 science flights with vertical profile sampling from 0.15 to 13 km from ~85° S to ~82° N (Thompson et al., 2022). The flight route of this extensive mission is presented in **Fig. 1**. To capture the seasonal variability of the atmosphere, these flight routes were performed once during each of the four seasons. The chemical composition of individual aerosols was measured using PALMS, which has been previously deployed for aircraft-based single-particle measurements (Thomson et al., 2000; Hudson et al., 2004; Liao et al., 2015). This mission is especially valuable for understanding the prevalence of ship exhaust particles because most of the measurements were made over the open ocean (**Fig. 1**).

In brief, PALMS is a single-particle mass spectrometer that uses a laser desorption ionization technique to characterize both non-refractory and refractory components of individual particles with diameters of 0.12 to 5 μm (Murphy et al., 2006). First, individual particles are introduced into the instrument by an aerosol-focusing inlet. Second, the single particles pass through two continuous beam lasers ($\lambda_{\text{max}} = 503 \text{ nm}$) and the resultant scattered light from both continuous lasers is used to determine the transit time of the particle, which can be used to calculate an aerodynamic diameter based on laboratory calibrations of size-selected polystyrene latex sphere standards (Duke Scientific). Third, the scattered light from the second continuous beam triggers a pulse from a 193 nm excimer laser, which ablates the particle and produces ions. Fourth, the generated ions pass

through a Time-of-Flight (ToF) mass spectrometer and are detected by their mass to charge ratio (m/z). During ATom, the polarity of the mass spectrometer was switched every few minutes to alternately detect negative and positive ions. In this work, we only use positive mass spectra, as vanadium is detected in this mode.

To classify the particles measured during ATom as PM from ship exhaust, we use spectral signatures of vanadium, nickel, iron, sulfate, and organics, which have been previously identified in single-particle mass spectrometry measurements in ship plumes near Rostock, Germany (Passig et al., 2021) and in the port of Los Angeles (Ault et al., 2010). In addition, we use empirical categories which are supported by clustering algorithms (Murphy et al., 2003) to categorize ship exhaust, biomass burning, mineral dust, sea salt, organic/sulfate/nitrate, and meteoric particle types by grouping similar mass spectra (Froyd et al., 2019). These categorizations are not perfect and can occasionally lead to the misidentification of one particle type for another; for example, both ship exhaust and mineral dust particles can contain vanadium (Adachi et al., 1997). To prevent misclassifying PM from ship emissions for mineral dust, we filter out particle spectra with high aluminum and silicon signatures (m/z of 27 and 28, respectively), which represent the major aluminosilicate component of mineral dust (Falkovich et al., 2001), relative to vanadium V^+ ($m/z = 51$), VO^+ ($m/z = 67$). Note that when we refer to sulfate and organics on ship exhaust particles, that is different than the total amount of particulate sulfate and organics from ships. Sulfate and organics from ship emissions also condense onto other particles and, as discussed in section 3.5, sulfate and organics from other sources can be added to ship exhaust particles during atmospheric aging.

The average mass spectra of identified vanadium-containing ship exhaust particles sampled in the MBL during the ATom campaign are presented in Fig. 2a. The MBL was defined using the definitions in Brock et al. (2021). Additional average mass spectra for this particle type as a function altitude are shown in **Fig. S1**. As shown in **Fig. 2a**, the average spectra appear similar across each ATom campaign, which suggests the composition of ship exhaust particles does not vary with season. For example, this particle type contains distinct spectral peaks, including V^+ ($m/z = 51$), VO^+ ($m/z = 67$), Ni^+ ($m/z = 58$), Fe^+ ($m/z = 56$), Na^+ ($m/z = 23$), S^+ ($m/z = 32$), SO^+ ($m/z = 48$), which is reflective of the chemical composition of heavy fuel oil (Ali and Abbas, 2006; Uhler et al., 2016). SO^+ at $m/z = 48$ can be distinguished from C_4^+ from soot by the absence of peaks such as C_3^+ and C_4H^+ . In addition, the mass spectra of our identified ship exhaust particles are in good agreement with those previously reported for single-particle mass spectrometry measurements taken in fresh ship plumes (Passig et al., 2021; Ault et al., 2010); however, in contrast to these studies, we observe a strong NO^+ ($m/z = 30$) signature. The strong NO^+ signals observed in this work may be a result of using a 193 nm excimer laser, which is more effective at ionizing nitrogen containing species compared to the 248 nm (Passig et al., 2021) and 266 nm laser (Ault et al., 2010) used in the other studies, which are more sensitive to iron and transition metals due to a resonance effect. Finally, this could also be indicative of atmospheric aging processes.

125 **2.2 Laboratory calibrations for vanadium**

To quantify vanadium in ship exhaust particles, we performed laboratory calibrations by nebulizing mixtures with known quantities of vanadium, sulfate, and organic compounds. We use the resultant aerosol as a proxy for PM emitted by ships and measure characteristic mass spectral signatures with PALMS. The calibration standards were prepared by dissolving varying

amounts of vanadium(IV) oxide sulfate hydrate ($\geq 99.99\%$; Sigma-Aldrich) and ammonium sulfate ($\geq 99.0\%$; Sigma-Aldrich) in deionized water (18 M Ω -cm) from a Millipore UV ultrapure water system. In cases where the organic content was varied in the calibration standards, a 1:1 mixture of sucrose (≥ 99.5 ; Sigma-Aldrich) and adipic acid ($\geq 99.0\%$; Gold Label, Aldrich) was used. These organic mixtures have been previously used in organic single-particle mass fraction calibrations for PALMS (Froyd et al. 2019). The solutions were aerosolized using laboratory-generated zero-air gas, which was fed into an Aeromist nebulizer.

As illustrated in **Fig. 2b**, the average mass spectra of the 0.1 wt % vanadium standard are representative of ambient ship exhaust particles measured during ATom, with the exception of Fe, Ni, K, and Na. To produce vanadium calibration curves, vanadium ion signals (V^+ and VO^+) were normalized to the sum of vanadium, organic (C^+ , CH^+ , CO^+ , and C_3^+), and sulfate (S^+ , SO^+ , and SO_2^+) ion signals from a suite of prepared standards. We include the organic and sulfate signals in the normalization because these species make up the bulk composition ($>95\%$) of primary PM emitted from heavy fuel oil combustion (Wu et al., 2018). The normalized vanadium signals for each calibration standard are then plotted as a function of known vanadium single-particle mass fraction in the standards to obtain a calibration curve (see **Fig. S2**). This range of vanadium content in the calibration curve (0.005 to 1.5 wt % in solution - 0.01-2 wt % normalized to sulfate and organics) is reflective of $> 85\%$ of the vanadium ion signals observed in ship exhaust particles from ambient measurements obtained during ATom (**Fig. 2b**).

To determine how efficiently vanadium is ionized within single particles, we obtain the relative ionization efficiency (RIE) of vanadium to organic and sulfate by fitting the calibration data with Eq. (1) equation presented by Froyd et al., 2019:

$$mf_v = \frac{m_v}{m_v + m_{org} + m_{sulf}} = \frac{sf_v}{\beta + sf_v(1 - \beta)} \quad (1)$$

Here, mf_v represents the single-particle mass fraction of vanadium, m_v is the mass of vanadium in a single particle, m_{org} is the mass of organics in a single particle, m_{sulf} is the mass of sulfate in a single particle, sf_v is the ion signal fraction of vanadium in a single particle, and β is the RIE of vanadium to organic and sulfate signals. In this work, we explore the RIE of vanadium for two conditions: 1) mixed vanadium(IV) oxide sulfate hydrate and ammonium sulfate solutions and 2) mixed vanadium(IV) oxide sulfate hydrate and ammonium sulfate with 20 wt % organics using a 1:1 sucrose to adipic acid mixture. These calibration curves were used to capture the range of vanadium, organic, and sulfate signals observed for ambient data (see **Fig. S2**).

As shown in **Fig. S1**, we obtain an RIE value for vanadium of ~ 340 for mixed vanadium(IV) oxide sulfate hydrate and ammonium sulfate and an RIE value for vanadium of ~ 126 for mixed vanadium(IV) oxide sulfate hydrate and ammonium sulfate with 20 wt % organics, which suggests the presence of organics can influence the ionization efficiency of vanadium in single particles. Conversely, vanadium can also alter the RIE of organics relative to sulfate (in comparison to pure organosulfate particles). Although these RIE variabilities broaden the uncertainty of the vanadium single-particle mass fractions, we apply an RIE of 330, which lies closer to the value obtained for pure vanadium(IV) oxide sulfate hydrate and/or ammonium sulfate mixed particles without added organics, as both our ambient data as well as previous aerosol mass

spectrometry studies have shown that accumulation mode ship exhaust particles are predominantly composed of sulfate (Murphy et al., 2009).

2.3 The application of laboratory calibrations to ATom data

165 The laboratory calibrations described above were applied to ATom data containing spectral signatures for ship exhaust particles (see **Section 2.1**) from the ATom data sets obtained for all four campaigns. In addition, only single-particle mass spectrometry measurements taken out-of-cloud were used in the calibrated data, as cloud droplets can produce particle artifacts (Murphy et al., 2004). Lastly, because land-based industrial processes (e.g., coal combustion and petroleum production) can produce vanadium-containing particles with similar mass spectra (Schlesinger et al., 2017), single-particle data obtained during ATom
170 were filtered for measurements taken over water. We also exclude data poleward of 65° N and 65° S because those regions are often ice-covered and not currently relevant for shipping.

The reported number of observed ship exhaust particles in the atmosphere depends on the criteria used to define this particle type (see **Section 2.1**). Using more stringent criteria will reduce the total number of ship exhaust particles observed in the atmosphere during ATom; however, this will also lead to fewer misclassifications of mass spectra that may marginally
175 resemble ship exhaust PM. In this work, we use strict criteria for the classification of ship exhaust particles, in which vanadium peak signals ($m/z = 51$ and 67) must be at least three times greater than the sum of the surrounding peak signals, as well as five and two times greater than aluminum and silicon peaks, respectively to remove potential mineral dust particles. We note that the application of this particle criteria results in a more conservative estimate for the number of ship exhaust particles measured during ATom. In addition, vanadium signals could be obscured by larger organic signals as particles age, although
180 the organic peaks do not get so large (section 3.5) for aging to obviously affect classification.

Despite this relatively strict definition for ship exhaust particles, we do not have confidence in the identification of ship exhaust particles during very high mineral dust loadings because some mineral dust particles contain vanadium with low aluminum and silicon ion signals. Therefore, we exclude measurements made in the Saharan Air Layer (SAL) dust region over the Atlantic, which ranges from -5° S to 30° N (-5-30° latitude) and 10° to 30° W (-10-30° longitude) depending on the season
185 (Tsamalis et al., 2013).

The largest factor that contributes to an underestimation of the reported number of ship exhaust particles in this study is the inability of PALMS to measure particles < 120 nm, which make up a significant component of ship exhaust particles (Zhou et al., 2019; Murphy et al., 2009). For example, Zhou and colleagues investigated the particle size distributions (10 nm to 10 μ m) of exhaust particles from various marine engines with different fuel types and observed that the majority of particles were <
190 100 nm in size. These ultrafine particles still make up a significant fraction of the total number of particles in plumes that are over an hour old (Murphy et al., 2009), which suggests that these particles likely exist long after a ship has passed.

3 Results and discussion

3.1 Ship exhaust particles are not limited to the marine boundary layer

As shown in **Fig. 3**, ~1% of accumulation mode particles ($d_p = 0.12\text{-}1\ \mu\text{m}$) measured by PALMS at altitudes $< 2\ \text{km}$ are particles emitted by ships. This percentage decreases with increasing altitude, which suggests that PM from ships is removed via wet deposition processes above the boundary layer. The removal of these particles via wet deposition is consistent with previous work by Coggon et al., 2012, who reported enhancements in both vanadium content in stratocumulus cloud water samples and cloud droplet number in marine air influenced by emissions from cargo and tanker ships. The processes and properties behind clouds formed by these ship exhaust particles (i.e., ship tracks) have been well documented in climate studies over the last several decades due to their indirect cooling effects from light scattering, which is suggested to reduce Earth's radiative forcing by $0.02\text{-}0.27\ \text{W m}^{-2}$ (Yuan et al., 2022).

Although ship exhaust particles play an important role in the formation of clouds, not all these particles are scavenged by water droplets during atmospheric convection. For example, vanadium-containing ship exhaust PM still makes up ~0.1% of the accumulation mode particles above 12 km (**Fig. 3**), which is approximately an order of magnitude lower than the number fractions measured in the marine boundary layer (MBL). Within the MBL, the highest number fraction of ship exhaust particles is in the Northern Hemisphere of the remote central Pacific and Atlantic Ocean between ~0 and ~50 degrees latitude (**Fig. 4a**), which is reflective of major shipping routes (Wu et al., 2017). At altitudes above the MBL, the number fraction of vanadium-containing ship exhaust particles decreases for both hemispheres (**Fig. 4b**). These results suggest that vanadium-containing ship exhaust particles are sufficiently widespread in the atmosphere. Each ~12° latitude bin in Figure 4 includes about 1000 to 4000 particles in the MBL and about 4000 to >10000 particles above the MBL during each deployment. With about 1% of particles in the MBL containing vanadium and less than that above the MBL, each point in **Fig. 4** represents tens of vanadium-containing particles.

It is important to mention that although ship exhaust plumes were not targeted during ATom, we encountered several sampling episodes of air heavily populated with vanadium-containing particles that were correlated with elevated numbers of black carbon, accumulation mode, and nucleation mode particles. These air masses also contained higher than background levels of NO_y and SO_2 mixing ratios, which suggests that we were likely sampling ship plumes. The encountered ship plumes appear to be somewhat dilute as they also contain particles from marine origin; for example, our data show that sea salt particles can contribute up to 60% of total measured single particles during these sampling periods. These dilute plume events can lead to unexpectedly noisy data when determining the widespread distribution of ship exhaust PM as one plume sampling episode can lead to an increase in the total fraction of vanadium-containing particles for a given area. For example, although the number fraction of vanadium-containing ship exhaust particles generally becomes more uniform above the MBL for a given hemisphere, these diluted plume events can lead to elevated number fractions within and above the MBL. This is particularly true for ATom 1, where the highest number of vanadium-containing particles in and above the MBL are observed at ~30° N

in both the Atlantic and Pacific Oceans (**Fig. 4**). This is a result of the aircraft sampling the same vanadium-enriched air masses at different altitudes during vertical profiling.

The diluted plume sampling events allow us to infer the fraction of ship exhaust particles that contain vanadium. During these episodes, organic/sulfate, sea salt, vanadium, and soot particles were all detected using PALMS. Aside from sea salt, these particle types have been previously identified in ship plumes (Ault et al., 2010). Using particle type fractions obtained from PALMS data during dilute plume measurements, we estimate that vanadium-containing particles can contribute anywhere from 10-40% of ship exhaust particles in the accumulation mode. This is in good agreement with Passig et al., 2021, who reported that 10-20% of particles during transient ship plume events off the coast of Rostock, Germany contained vanadium.

3.2 Vanadium content of individual ship exhaust particles

As shown in **Fig. S4** and **S5**, ship exhaust particles can have over an order of magnitude difference in vanadium content with most of the particles containing < 2 wt % vanadium. In addition, the highest vanadium single-particle mass fractions are observed in the MBL compared to the free troposphere (**Fig. 3**). Since vanadium is stable in the particle phase, we do not expect the absolute amount of vanadium to change as a function of altitude. Instead, these results indicate that ship exhaust particles experience atmospheric aging through the accumulation of non-vanadium species, which would reduce the contribution of the vanadium ion signals to the total ion signals obtained for individuals and lead to lower vanadium single-particle mass fractions. Further discussion on the atmospheric processing of ship exhaust particles is discussed in **Section 3.4**.

The vanadium single-particle mass fractions in the Pacific and Atlantic Oceans in the northern hemisphere 20° N to 65° N (20 to 65° latitude), tropics 20° S to 20° N (-20 to 20° latitude), and southern hemisphere 20° S to 65° S (-20 to -65° latitude) are presented in **Fig. 5**. The vanadium single-particle mass fractions in this figure are obtained from the average vanadium content of all the ship exhaust particles sampled in a given area (i.e., northern hemisphere, tropics, and southern hemisphere). We measure the highest average vanadium single-particle mass fraction for particles sampled in the tropical Pacific during summer compared to other locations and seasons. The majority of particles measured in this tropical Pacific region were sampled from a single plume event that contained higher than average vanadium ion signals measured throughout ATom. These vanadium single-particle mass fractions are also higher than those measured in other ship plume events, which may be attributed to this particular ship using a fuel that contained more heavy metal impurities or having different engine operating conditions.

3.3 Ship exhaust particles are rich in sulfate and lower in organic matter, ammonium and nitrate

To determine the organic and sulfate single-particle mass fractions in individual ship exhaust particles, we apply the organic and sulfate calibrations discussed in **Section 2.2**. As illustrated in **Fig. 6**, ship exhaust particles contain more than 80% sulfate. These results agree with previous studies investigating the chemical composition of ship exhaust particles (Ault et al., 2010; Murphy et al., 2009; Healy et al., 2009; Agrawal et al., 2008); for example, using aircraft-based aerosol mass spectrometer measurements on the Twin Otter, Murphy and colleagues determined that ship exhaust particles contain over 70 wt % sulfate (Murphy et al., 2009). The slightly higher sulfur content presented in this work may be attributed to variations in plume ages

as the measurements did not specifically target recently emitted ship plumes. The dominant sulfate fraction of ship exhaust particles determined from in-situ measurements is compositionally different from the heavy fuel oils used in marine vessels, which are predominantly composed of organic material and only up to a few wt % sulfur (Uhler et al., 2016). This chemical difference has been attributed to the aqueous oxidation of SO₂, a major gas-phase pollutant emitted during ship fuel
260 combustion, to particle-phase sulfate and sulfuric acid (Healy et al., 2009; Murphy et al., 2009). The aqueous-phase oxidation of SO₂ in the atmosphere is suggested to happen quickly (Finlayson-Pitts and Pitts Jr., 1999), which explains why ship exhaust particles measured in fresh plumes are still sulfate-rich (Murphy et al., 2009). Finally, previous studies have demonstrated that vanadium can participate in the catalytic oxidation of SO₂ (Barbaray et al., 1978). Similar catalytic oxidation mechanisms may also be true for other transition metals in ship exhaust particles, including iron (Fu et al., 2007).

265 Although sulfate is the dominant component of the vanadium-containing ship exhaust particles measured in this study, there is still < 20 wt % organic component. Similar to previous aerosol and single-particle mass spectrometer measurements (Liu et al., 2022), the organic fraction of ship exhaust particles appears to be relatively oxidized throughout ATom. For example, indicators of oxidized organics (e.g., CO⁺, C₂H₃O⁺) do not vary with altitude. Furthermore, these signals appear similar for in and out of dilute plume measurements, which suggests the majority of organic oxidation occurs relatively quickly. These
270 results agree with the single-particle aerosol mass spectrometer measurements made offshore of the East China Sea, which demonstrated high degrees of oxidation for vanadium-containing ship exhaust particles (Liu et al., 2022). We also observe oxidized organic ion signals in non-vanadium-containing ship exhaust particles; for example, both organic/sulfate and soot particles measured in dilute plume events during ATom often displayed CO⁺ ion signals in their mass spectra.

As illustrated in **Fig. 2**, ammonium ion signals (NH₄⁺) were consistently detected in ship exhaust in single-particle mass spectra
275 of ship exhaust particles during ATom. Ammonium has been previously reported in ship exhaust particles and is a secondary species that is formed from the reaction of ammonia with sulfuric acid that is formed during SO₂ oxidation (Ault et al., 2010). The PALMS instrument detects neutralized and incompletely neutralized sulfuric acid in positive ions as SO⁺ and H₃SO₄H⁺. During ATom, we detect both SO⁺ and H₃SO₄H⁺ in vanadium-containing particles, which is consistent with incomplete neutralization of a substantial sulfate/sulfuric acid content with ammonia. Using the NH₄⁺ ion signal from laboratory
280 calibrations, we estimate that vanadium-containing ship exhaust particles measured during ATom contain less than 16 wt % of ammonium.

Although NO⁺ signals can be produced from ammonium during laser ablation, it is also formed from nitrate; therefore, ammonium may not be entirely responsible for the NO⁺ ion signal observed in ambient spectra. In fact, nitrate has been
285 previously measured in ship exhaust particles near ports (Healy et al., 2009) and in ship plumes (Murphy et al., 2009) and is thought to be formed by secondary reaction mechanisms. The formation of particulate-phase nitrate in aged ship exhaust particles has been explained by ozone oxidation of NO_x from a field study conducted at a port in Shanghai China (Wang et al., 2019). In this work, the authors used wind diagrams to determine fresh and aged particles from ship plumes and found that aged particles contained higher nitrate ion signals in regions of depleted ozone mixing ratios. Although ozone measurements were made during ATom, it is difficult to correlate the nitrate content of ship exhaust particles with ozone mixing ratios, as

290 ozone becomes depleted in the MBL due to ocean surface deposition and entrainment in sea spray aerosol (Singh et al., 1996). Nitrate can also form on ship exhaust particles via the direct reduction of NO_x through catalytic heterogeneous chemistry with vanadium and other multi-valent metals (e.g., iron, nickel), which will be discussed in more detail in the next section (**Section 3.4**).

3.4 Metal catalysis in ship exhaust particles

295 Many of the metals generated during the combustion of heavy fuel oil are multivalent (e.g., vanadium, nickel, and iron) (Corbin et al., 2018), which means they have the potential to participate in redox reactions with other atmospheric pollutants. For example, nitrate formation has been previously observed during NO_x uptake by mineral dust and mineral dust proxies (i.e., metal oxides) (Underwood et al., 1999). The metals in ship exhaust particles may similarly undergo redox chemistry with NO_x to lead to the production of particulate nitrate. Furthermore, if vanadium, iron, and nickel are present in their semiconducting

300 metal oxide forms (i.e., V_2O_5 , NiO , Fe_2O_3) then their optical band gaps would lie within the UV/visible region of the solar spectrum (Beke, 2011; Hosny, 2011; Al-Gaashani et al., 2013), which could lead to photoenhanced decomposition of NO_2 and the subsequent formation of nitrate. This photochemical transformation has been previously observed for mineral dust and metal oxides (Ndour et al., 2009, 2008; Chen et al., 2011); however, we note that the chemistry of the metal species in ship exhaust particles may be different than that of mineral dust, as their chemical form and solubility is not well understood.

305 Similarly, particulate sulfate can be formed via the heterogeneous chemistry of transition metals with SO_2 . For example, work by Barbaray and coworkers demonstrated that vanadium pentoxide particles can catalyze the oxidation of SO_2 into particle-phase sulfate in the presence of H_2O and NO_2 (Barbaray et al., 1978). This catalytic oxidation mechanism has been previously hypothesized to occur in PM emitted by ships (Murphy et al., 2009; Ault et al., 2010) and was further supported by a study that determined vanadium pentoxide to be the dominant vanadium species of fine PM in diesel exhaust (Shafer et al., 2012).

310 Similarly, iron and manganese have been found to catalyze the oxidation of SO_2 (Hoffmann and Jacob, 1984) and are suggested to be responsible for 9-17% of global sulfate production (Alexander et al., 2009).

Transition metal ion catalyzed reactions with H_2O_2 in aqueous particles can lead to the formation of reactive oxygen species (ROS), including the hydroxyl radical (OH) and peroxy radical (HO_2) (Lousada et al., 2012; Enami et al., 2014). This Fenton or Fenton-like chemistry is suggested to play an important role in H_2O_2 atmospheric budget and can influence the oxidative

315 capacity of the atmosphere. Iron is the most important transition metal for controlling the OH, HO_2 , H_2O_2 budget and is thought to be the main driver of H_2O_2 uptake in ambient aerosols (Qin et al., 2022). This ROS budget is thought to be controlled by the number concentration of iron-containing particles rather than the total iron mass fraction (Khaled et al., 2022), which highlights the importance of single-particle chemical analysis for determining the oxidative capacity of the atmosphere. Although this study focused on iron-catalyzed chemistry with H_2O_2 , vanadium-containing ship exhaust particles almost always

320 contain iron (Healy et al., 2009) and could provide clues to the importance of Fenton chemistry for ship exhaust particles. Finally, other transition metals, including copper (Song et al., 2020) and vanadium (Mizuno and Kamata, 2011) have also been

found to react with H_2O_2 to produce ROS. Given the prevalence of metals in ship exhaust particles, it is reasonable to assume that these particles can also facilitate the formation of ROS species through interaction with H_2O_2 .

3.5 Vanadium-containing ship exhaust particles experience atmospheric aging

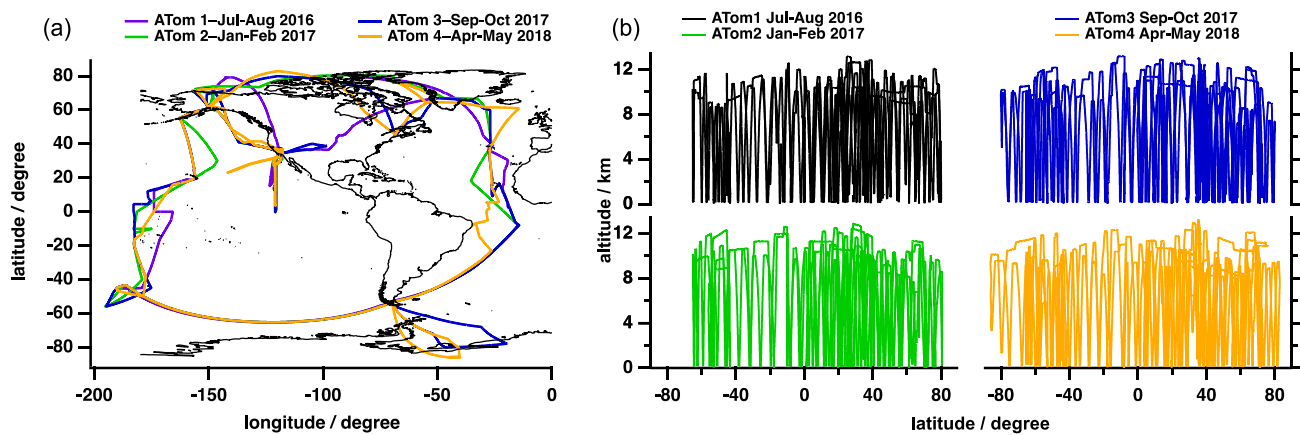
325 As described above, the vanadium single-particle mass fractions calculated in this work were normalized to the sum of the vanadium, sulfate, and organic signals (see **Section 2.2**); therefore, a decrease in vanadium single-particle mass fraction must be correlated with an increase in the organic and/or sulfate ion signals. As shown in **Fig. 6**, we observe an increase in the sulfate single-particle mass fraction in ship exhaust particles with increasing altitude, which suggests ship exhaust particles continue to accumulate sulfate during their atmospheric lifetime. These results are in good agreement with those presented by
330 Murphy and coworkers, who observed a gradual increase in sulfate mass fractions of ship exhaust particles as a function of plume age using an aerosol mass spectrometer (Murphy et al., 2009). However, we do not expect this few wt % increase in sulfur single-particle mass fraction observed during atmospheric aging to significantly impact the cloud droplet activation properties of these particles as they are predominantly composed of sulfate immediately after emission (Murphy et al., 2009). As illustrated in **Fig. 7**, the NO^+ signal measured for individual ship exhaust particles increases as a function of altitude.
335 Previous studies have associated nitrate in ship exhaust particles with more aged particles (Wang et al., 2019; Passig et al., 2021). Although we did not attempt to quantify nitrate single-particle mass fractions in individual ship exhaust particles in this work, Murphy and coworkers determined that nitrate in the non-refractory dry component of ship exhaust particles increased up to 1 wt % in plumes that were over an hour old (Murphy et al., 2009).

4 Conclusion

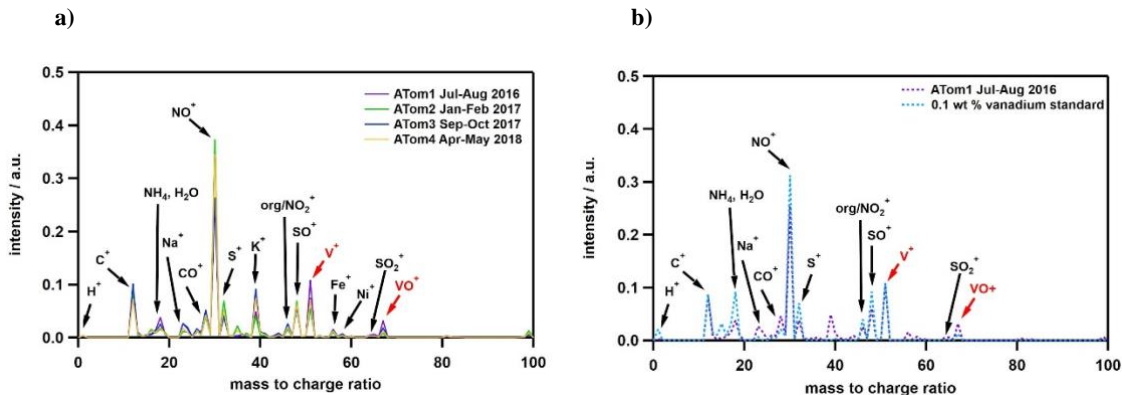
340 In this study, we report that ~1 % of particles measured in the MBL over the remote Atlantic and Pacific are vanadium-containing particles from ship emissions from measurements that did not target ship plumes. In addition, we use laboratory calibrations to determine that the majority of these particles contain less than 2 wt % vanadium but that the single-particle mass fractions in individual particles can vary over an order of magnitude. Furthermore, we demonstrate that these particles are predominantly made up of sulfate (> 80 wt %) and continue to accumulate sulfate, as well as nitrate during atmospheric
345 aging. Finally, we note that there are likely more vanadium-containing particles that are smaller than the lower size limit of our measurements, which may lead us to underestimate the fraction of particles in the marine atmosphere.

Although vanadium-containing ship exhaust particles are primarily composed of sulfate, the few wt % or less of vanadium in these particles can influence catalytic heterogeneous chemistry and photochemistry of ship exhaust particles, which can change their chemical composition and cloud formation properties. For example, vanadium-based catalysts have been explored as a
350 commercial material for denitrification of NO_x in combustion plumes (Chen et al., 2018). These catalysts have been shown to be effective in removing NO_x with less than 1 wt % of vanadium. Despite the powerful catalytic capabilities of vanadium and

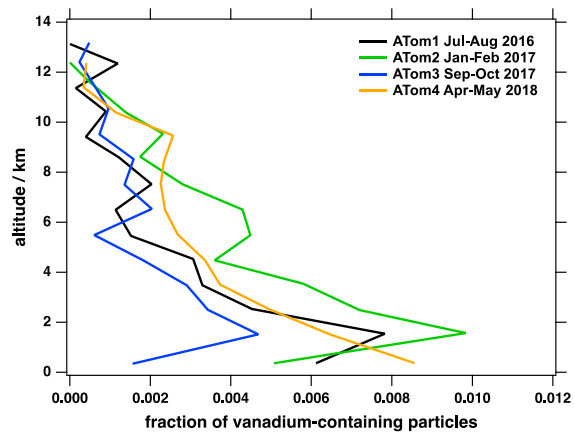
other transition metals, it is difficult to determine how much of the nitrate and sulfate accumulation in ship exhaust particles is attributed to redox chemistry with these metallic species versus other aqueous phase oxidation reaction mechanisms. Finally, we note that the measurements presented in this work were conducted before the International Maritime Organization's Sulfur 2020 policy, which required the shipping industry to transition from 3.5% to 0.5% m/m sulfur-containing fuel. This policy, which has demonstrated effectiveness in decreasing SO₂ emissions from the Maritime Industry (Kim et al., 2022; Song et al., 2022), may also alter the current distribution and single-particle mass fractions of vanadium in ship exhaust particles. For example, Yu and colleagues reported significant reductions in vanadium loadings from bulk ship PM measurements conducted after Sulfur 2020 (Yu et al., 2021); however, vanadium is still frequently detected in ship exhaust particles emitted during the combustion of low sulfur fuels (Zhou et al., 2020). It is currently not clear how low sulfur fuels impact the vanadium content on an individual particle level and whether the single-particle mass fractions are still sufficiently large for ship particles to participate in catalytic heterogeneous chemistry and cloud droplet activation.



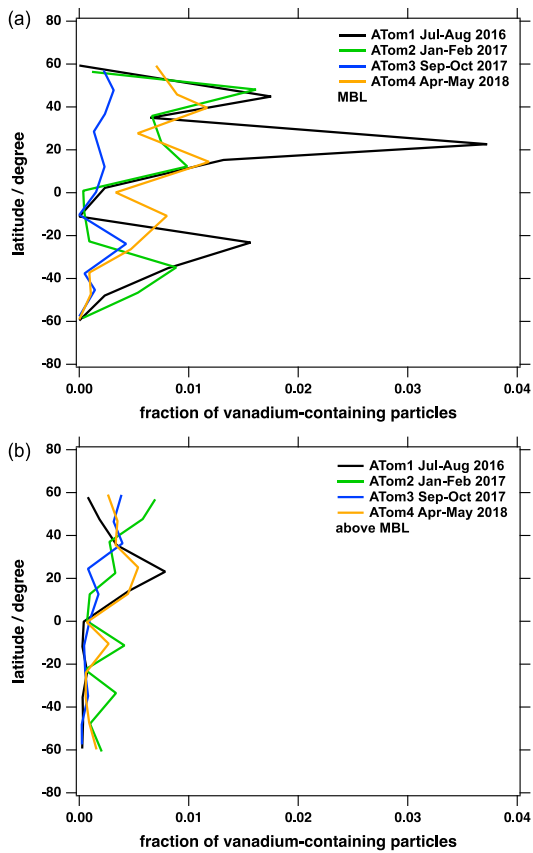
365 **Figure 1:** a) The flight route of the NASA DC-8 aircraft during each of the four ATom campaigns and b) sampling altitudes as a function of latitude during ATom. Each colored line represents the flight path and altitude taken for a given campaign.



370 **Figure 2:** Mass spectra degraded to unit mass resolution for average mass spectra comparisons of vanadium-containing ship exhaust particles measured in the MBL a) during all ATom campaigns b) during ATom 1 with a 0.1 wt % vanadium calibration standard. Only similar peaks between ATom and the calibration standard are labeled. The standard was a mixture containing vanadium sulfate, ammonium sulfate, and trace organics. The V^+ peak for ATom 1 is difficult to see due to overlap with the calibration standard.



375 **Figure 3:** Fraction of vanadium-containing particles as a function of altitude. Each colored line represents a different ATom campaign with 20 particle averages.



380 **Figure 4:** Fraction of vanadium-containing particles as a function of latitude in a) the MBL and b) above the MBL. Each colored line represents a different ATom campaign and oceanic region with 20 particle averages. We note that the fraction of vanadium-containing particles presented below exclude measurements taken in the Saharan Air Layer off the west coast of Africa to filter out vanadium-containing mineral dust particles. In addition, we exclude measurements made above 65° N and below 65° S to remove polar regions, which lack ship traffic and where pack ice can change the type of boundary layer.

385

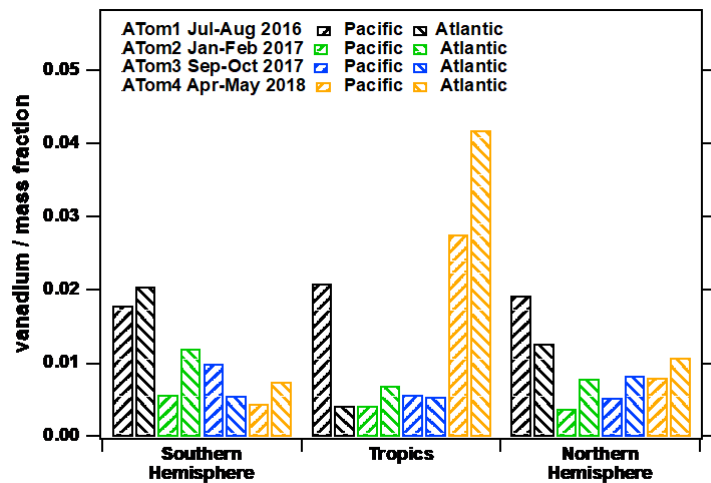


Figure 5: Average vanadium mass fractions in vanadium-containing ship exhaust particles measured in the Northern Hemisphere (20° N to 65° N; 20 to 65° latitude), Tropics (20° S to 20° N; -20 to 20° latitude), and Southern Hemisphere (20° S to 65° S; -20 to -65° latitude) in the Atlantic and Pacific Ocean for all four ATom at all sampling altitudes. The vanadium mass fraction in all aerosol is much smaller, roughly these mass fractions times the fractions of vanadium-containing particles (Figure 4).

390

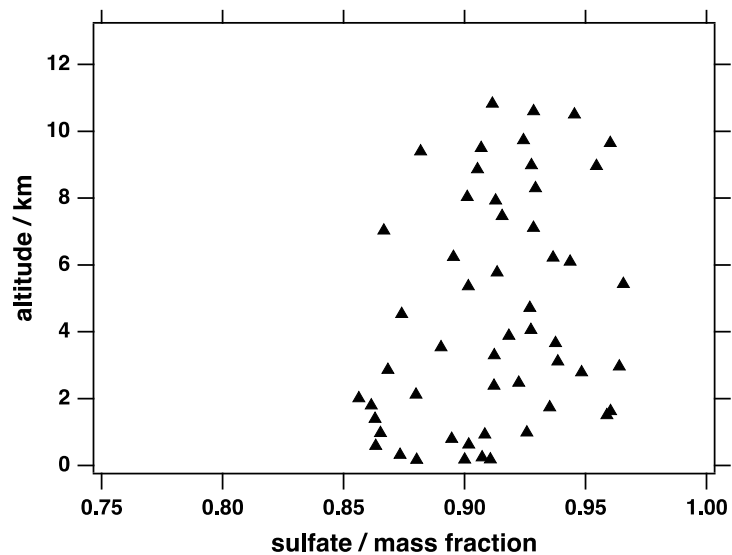


Figure 6: Sulfate mass fractions in vanadium-containing ship exhaust particles as a function of altitude for ATom 1-4. Each point represents 20 particle averages. There were no obvious differences between the ATom campaigns for this figure.

395

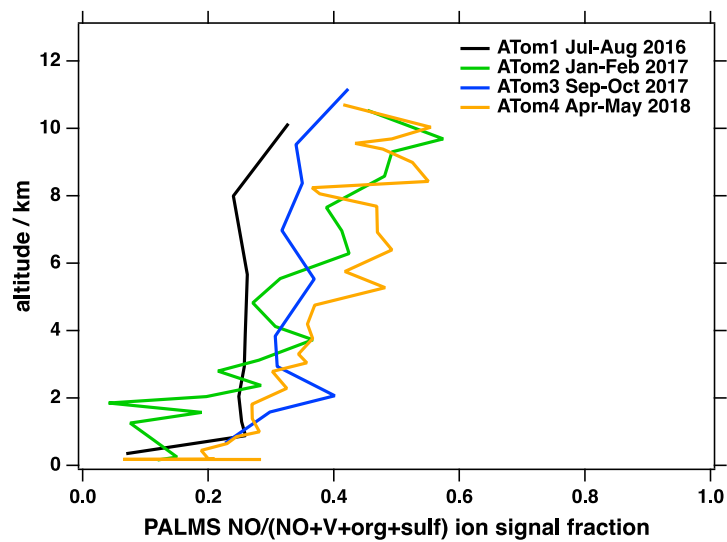


Figure 7: NO^+ ion signals as a function of altitude for vanadium-containing ship exhaust particles measured during ATom. Each colored line represents a different ATom campaign with 20 particle averages.

Data Availability

Data are publicly available at https://daac.ornl.gov/ATOM/guides/ATom_merge.html.

Supplement

Author contributions

405 M.A-G. conducted laboratory aerosol calibrations with assistance from M.J.L. M.A-G. performed data analysis and wrote the manuscript with critical comments from D.M.M, G.P.S, M.J.L., and K. D. F. PALMS data was collected during research flights by D.M.M., G.P.S, and K.D.F.

Competing interests

The authors declare no competing interests.

410 Acknowledgements

M.A-G. held an NRC Research Associateship award at NOAA Chemical Sciences Laboratory.

Financial support

The Atmospheric Tomography Missions were supported by NASA's Earth System Science Pathfinder Program EVS-2 funding. Research flight participation for D.M.M., G.P.S, and K.D.F was supported by NOAA climate funding and NASA
415 (no. NNH15AB12I). NOAA cooperative agreement NA17OAR4320101 supported G.P.S., K.D.F., and M.J.L. NOAA cooperative agreement NA22OAR4320151 supported G.P.S. and M.J.L. An NRC Research Associateship award at NOAA Chemical Sciences Laboratory was held by M.A-G.

References

- 420 Adachi, A., Ogawa, K., Tsushi, Y., Nagao, N., and Kobayashi, T.: Determination of vanadium in environmental samples by atomic absorption spectrophotometry, *Water Res.*, 31, 1247–1250, [https://doi.org/10.1016/S0043-1354\(96\)00379-X](https://doi.org/10.1016/S0043-1354(96)00379-X), 1997.
- Agrawal, H., Malloy, Q. G. J., Welch, W. A., Wayne Miller, J., and Cocker, D. R.: In-use gaseous and particulate matter emissions from a modern ocean going container vessel, *Atmos. Environ.*, 42, 5504–5510, <https://doi.org/10.1016/j.atmosenv.2008.02.053>, 2008.
- 425 Alexander, B., Park, R. J., Jacob, D. J., and Gong, S.: Transition metal-catalyzed oxidation of atmospheric sulfur: Global implications for the sulfur budget, *J. Geophys. Res. Atmos.* 114(D2), <https://doi.org/10.1029/2008JD010486>, 2009.
- Al-Gaashani, R., Radiman, S., Tabet, N., and Daud, A. R.: Rapid synthesis and optical properties of hematite (α -Fe₂O₃) nanostructures using a simple thermal decomposition method, *J. Alloys Compd.*, 550, 395–401, <https://doi.org/10.1016/j.jallcom.2012.10.150>, 2013.
- 430 Ali, M. F. and Abbas, S.: A review of methods for the demetallization of residual fuel oils, *Fuel Process. Technol.*, 87, 573–584, <https://doi.org/10.1016/j.fuproc.2006.03.001>, 2006.
- 435 Anders, L., J. Schade, E. I. Rosewig, T. Kröger-Badge, R. Irsig, S. Jeong, J. Bendl, M. R. Saraji-Bozorgzad, J.-H. Huang, F.-Y. Zhang, C. C. Wang, T. Adam, M. Sklorz, U. Etzien, B. Buchholz H. Czech, T. Streibel, J. Passig, and R. Zimmermann, Detection of ship emissions from distillate fuel operation via single-particle profiling of polycyclic aromatic hydrocarbons, *Environ. Sci.: Atmos.*, 3, 1134, [10.1039/d3ea00056g](https://doi.org/10.1039/d3ea00056g), 2023.
- 440 IMO 2020 – cutting sulphur oxide emissions: <https://www.imo.org/en/MediaCentre/HotTopics/Pages/Sulphur-2020.aspx>, last access: 14 July 2023.
- Ault, A. P., Gaston, C. J., Wang, Y., Dominguez, G., Thiemens, M. H., and Prather, K. A.: Characterization of the Single Particle Mixing State of Individual Ship Plume Events Measured at the Port of Los Angeles, *Environ. Sci. Technol.*, 44, 1954–1961, <https://doi.org/10.1021/es902985h>, 2010.
- 445 Barbaray, B., Contour, J. P., and Mouvier, G.: Effects of nitrogen dioxide and water vapor on oxidation of sulfur dioxide over vanadium pentoxide particles, *Environ. Sci. Technol.*, 12, 1294–1297, <https://doi.org/10.1021/es60147a012>, 1978.
- 450 Beke, S.: A review of the growth of V₂O₅ films from 1885 to 2010, *Thin Solid Films*, 519, 1761–1771, <https://doi.org/10.1016/j.tsf.2010.11.001>, 2011.
- Bollati, V., Marinelli, B., Apostoli, P., Bonzini, M., Nordio, F., Hoxha, M., Pegoraro, V., Motta, V., Tarantini, L., Cantone, L., Schwartz, J., Bertazzi, P. A., and Baccarelli, A.: Exposure to Metal-Rich Particulate Matter Modifies the Expression of Candidate MicroRNAs in Peripheral Blood Leukocytes, *Environ. Health Perspect.*, 118, 763–768, <https://doi.org/10.1289/ehp.0901300>, 2010.
- 455 Brock, C. A., K. D. Froyd, M. Dollner, C. J. Williamson, G. Schill, D. M. Murphy, N. J. Wagner, A. Kupc, J. L. Jimenez, P. Campuzano-Jost, B. A. Nault, J. C. Schroder, D. A. Day, D. J. Price, B. Weinzierl, J. P. Schwarz, J. M. Katich, S. Wang, L. Zeng, R. Weber, J. Dibb, E. Scheuer, G. S. Diskin, J. P. DiGangi, T.P. Bui, J. M. Dean-Day., C. R. Thompson, J. Peischl, T. B. Ryerson, I. Bourgeois, B. C. Daube, R. Commane, and S. C. Wofsy, Ambient aerosol properties in the remote atmosphere from global-scale in situ measurement. *Atmos. Chem. Phys.*, 21, 15023–15063, <https://doi.org/10.5194/acp-21-15023-2021>, 2021.
- 460
- 465

- Celo, V., Dabek-Zlotorzynska, E., and McCurdy, M.: Chemical Characterization of Exhaust Emissions from Selected Canadian Marine Vessels: The Case of Trace Metals and Lanthanoids, *Environ. Sci. Technol.*, 49, 5220–5226, <https://doi.org/10.1021/acs.est.5b00127>, 2015.
- 470 Chen, C., Cao, Y., Liu, S., Chen, J., and Jia, W.: Review on the latest developments in modified vanadium-titanium-based SCR catalysts, *Chin. J. Catal.*, 39, 1347–1365, [https://doi.org/10.1016/S1872-2067\(18\)63090-6](https://doi.org/10.1016/S1872-2067(18)63090-6), 2018.
- Chen, H., Navea, J. G., Young, M. A., and Grassian, V. H.: Heterogeneous Photochemistry of Trace Atmospheric Gases with Components of Mineral Dust Aerosol, *J. Phys. Chem. A*, 115, 490–499, <https://doi.org/10.1021/jp110164j>, 2011.
- 475 Coggon, M. M., Sorooshian, A., Wang, Z., Metcalf, A. R., Frossard, A. A., Lin, J. J., Craven, J. S., Nenes, A., Jonsson, H. H., Russell, L. M., Flagan, R. C., and Seinfeld, J. H.: Ship impacts on the marine atmosphere: insights into the contribution of shipping emissions to the properties of marine aerosol and clouds, *Atmospheric Chem. Phys.*, 12, 8439–8458, <https://doi.org/10.5194/acp-12-8439-2012>, 2012.
- 480 Corbett, J. J., Winebrake, J. J., Green, E. H., Kasibhatla, P., Eyring, V., and Lauer, A.: Mortality from Ship Emissions: A Global Assessment, *Environ. Sci. Technol.*, 41, 8512–8518, <https://doi.org/10.1021/es071686z>, 2007.
- Corbin, J. C., Mensah, A. A., Pieber, S. M., Orasche, J., Michalke, B., Zanatta, M., Czech, H., Massabò, D., Buatier de
485 Mongeot, F., Mennucci, C., El Haddad, I., Kumar, N. K., Stengel, B., Huang, Y., Zimmermann, R., Prévôt, A. S. H., and Gysel, M.: Trace Metals in Soot and PM_{2.5} from Heavy-Fuel-Oil Combustion in a Marine Engine, *Environ. Sci. Technol.*, 52, 6714–6722, <https://doi.org/10.1021/acs.est.8b01764>, 2018.
- Enami, S., Sakamoto, Y., and Colussi, A. J.: Fenton chemistry at aqueous interfaces, *Proc. Natl. Acad. Sci.*, 111, 623–628,
490 <https://doi.org/10.1073/pnas.1314885111>, 2014.
- Eyring, V., Köhler, H. W., van Aardenne, J., and Lauer, A.: Emissions from international shipping: 1. The last 50 years, *J. Geophys. Res. Atmos.*, 110(D17), <https://doi.org/10.1029/2004JD005619>, 2005.
- 495 Falkovich, A. H., Ganor, E., Levin, Z., Formenti, P., and Rudich, Y.: Chemical and mineralogical analysis of individual mineral dust particles, *J. Geophys. Res. Atmospheres*, 106, 18029–18036, <https://doi.org/10.1029/2000JD900430>, 2001.
- Finlayson-Pitts, B. J. and Pitts Jr., J. N.: *Chemistry of the Upper and Lower Atmosphere: Theory, Experiments, and Applications*, Elsevier, 1999.
- 500 Froyd, K. D., Murphy, D. M., Brock, C. A., Campuzano-Jost, P., Dibb, J. E., Jimenez, J.-L., Kupc, A., Middlebrook, A. M., Schill, G. P., Thornhill, K. L., Williamson, C. J., Wilson, J. C., and Ziemba, L. D.: A new method to quantify mineral dust and other aerosol species from aircraft platforms using single-particle mass spectrometry, *Atmos. Meas. Tech.*, 12, 6209–6239, <https://doi.org/10.5194/amt-12-6209-2019>, 2019.
- 505 Fu, H., Wang, X., Wu, H., Yin, Y., and Chen, J.: Heterogeneous Uptake and Oxidation of SO₂ on Iron Oxides, *J. Phys. Chem. C*, 111, 6077–6085, <https://doi.org/10.1021/jp070087b>, 2007.
- 510 Healy, R. M., O'Connor, I. P., Hellebust, S., Allanic, A., Sodeau, J. R., and Wenger, J. C.: Characterisation of single particles from in-port ship emissions, *Atmos. Environ.*, 43, 6408–6414, <https://doi.org/10.1016/j.atmosenv.2009.07.039>, 2009.

- 515 Hobbs, P. V., Garrett, T. J., Ferek, R. J., Strader, S. R., Hegg, D. A., Frick, G. M., Hoppel, W. A., Gasparovic, R. F., Russell, L. M., Johnson, D. W., O'Dowd, C., Durkee, P. A., Nielsen, K. E., and Innis, G.: Emissions from Ships with respect to Their Effects on Clouds, *J. Atmospheric Sci.*, 57, 2570–2590, [https://doi.org/10.1175/1520-0469\(2000\)057<2570:EFSWRT>2.0.CO;2](https://doi.org/10.1175/1520-0469(2000)057<2570:EFSWRT>2.0.CO;2), 2000.
- 520 Hoffmann, M. and Jacob, D. J.: Kinetics and Mechanism of the Catalytic Oxidation of Sulfur Dioxide in Aqueous Solution: Application to Nighttime Fog and Cloud Water Chemistry, Butterworth Publishers, Boston, MA, 101–172, 1984.
- Hosny, N. M.: Synthesis, characterization and optical band gap of NiO nanoparticles derived from anthranilic acid precursors via a thermal decomposition route, *Polyhedron*, 30, 470–476, <https://doi.org/10.1016/j.poly.2010.11.020>, 2011.
- 525 Hudson, P. K., Murphy, D. M., Cziczo, D. J., Thomson, D. S., de Gouw, J. A., Warneke, C., Holloway, J., Jost, H.-J., and Hübner, G.: Biomass-burning particle measurements: Characteristic composition and chemical processing, *J. Geophys. Res. Atmos.*, 109, <https://doi.org/10.1029/2003JD004398>, 2004.
- 530 Khaled, A., Zhang, M., and Ervens, B.: The number fraction of iron-containing particles affects OH, HO₂ and H₂O₂ budgets in the atmospheric aqueous phase, *Atmospheric Chem. Phys.*, 22, 1989–2009, <https://doi.org/10.5194/acp-22-1989-2022>, 2022.
- Kim, Y., Moon, N., Chung, Y., and Seo, J.: Impact of IMO Sulfur Regulations on Air Quality in Busan, Republic of Korea, *Atmos.*, 13, 1631, <https://doi.org/10.3390/atmos13101631>, 2022.
- 535 Lauer, A., Eyring, V., Hendricks, J., Jöckel, P., and Lohmann, U.: Global model simulations of the impact of ocean-going ships on aerosols, clouds, and the radiation budget, *Atmos. Chem. Phys.*, 7, 5061–5079, <https://doi.org/10.5194/acp-7-5061-2007>, 2007.
- 540 Lehtoranta, K., Aakko-Saksa, P., Murtonen, T., Vesala, H., Ntziachristos, L., Rönkkö, T., Karjalainen, P., Kuittinen, N., and Timonen, H.: Particulate Mass and Nonvolatile Particle Number Emissions from Marine Engines Using Low-Sulfur Fuels, Natural Gas, or Scrubbers, *Environ. Sci. Technol.*, 53, 3315–3322, <https://doi.org/10.1021/acs.est.8b05555>, 2019.
- 545 Liao, J., Froyd, K. D., Murphy, D. M., Keutsch, F. N., Yu, G., Wennberg, P. O., St. Clair, J. M., Crouse, J. D., Wisthaler, A., Mikoviny, T., Jimenez, J. L., Campuzano-Jost, P., Day, D. A., Hu, W., Ryerson, T. B., Pollack, I. B., Peischl, J., Anderson, B. E., Ziemba, L. D., Blake, D. R., Meinardi, S., and Diskin, G.: Airborne measurements of organosulfates over the continental U.S., *J. Geophys. Res. Atmos.*, 120, 2990–3005, <https://doi.org/10.1002/2014JD022378>, 2015.
- 550 Liu, Z., Chen, H., Li, L., Xie, G., Ouyang, H., Tang, X., Ju, R., Li, B., Zhang, R., and Chen, J.: Real-time single particle characterization of oxidized organic aerosols in the East China Sea, *NPJ Clim. Atmos. Sci.*, 5, 1–9, <https://doi.org/10.1038/s41612-022-00267-1>, 2022.
- Lousada, C. M., Johansson, A. J., Brinck, T., and Jonsson, M.: Mechanism of H₂O₂ Decomposition on Transition Metal Oxide Surfaces, *J. Phys. Chem. C*, 116, 9533–9543, <https://doi.org/10.1021/jp300255h>, 2012.
- 555 Mizuno, N. and Kamata, K.: Catalytic oxidation of hydrocarbons with hydrogen peroxide by vanadium-based polyoxometalates, *Coord. Chem. Rev.*, 255, 2358–2370, <https://doi.org/10.1016/j.ccr.2011.01.041>, 2011.
- 560 Moldanová, J., Fridell, E., Winnes, H., Holmin-Fridell, S., Boman, J., Jedynska, A., Tishkova, V., Demirdjian, B., Joulie, S., Bladt, H., Ivleva, N. P., and Niessner, R.: Physical and chemical characterisation of PM emissions from two ships operating in European Emission Control Areas, *Atmos. Meas. Tech.*, 6, 3577–3596, <https://doi.org/10.5194/amt-6-3577-2013>, 2013.

- Moreno, T., Querol, X., Alastuey, A., de la Rosa, J., Sánchez de la Campa, A. M., Minguillón, M., Pandolfi, M., González-Castanedo, Y., Monfort, E., and Gibbons, W.: Variations in vanadium, nickel and lanthanoid element concentrations in urban air, *Sci. Total Environ.*, 408, 4569–4579, <https://doi.org/10.1016/j.scitotenv.2010.06.016>, 2010.
- 565 Murphy, D. M., Middlebrook, A. M., and Warshawsky, M.: Cluster Analysis of Data from the Particle Analysis by Laser Mass Spectrometry (PALMS) Instrument, *Aerosol Sci. Technol.*, 37, 382–391, <https://doi.org/10.1080/02786820300971>, 2003.
- 570 Murphy, D. M., Cziczo, D. J., Hudson, P. K., Thomson, D. S., Wilson, J. C., Kojima, T., and Buseck, P. R.: Particle Generation and Resuspension in Aircraft Inlets when Flying in Clouds, *Aerosol Sci. Technol.*, 38, 401–409, <https://doi.org/10.1080/02786820490443094>, 2004.
- 575 Murphy, D. M., Cziczo, D. J., Froyd, K. D., Hudson, P. K., Matthew, B. M., Middlebrook, A. M., Peltier, R. E., Sullivan, A., Thomson, D. S., and Weber, R. J.: Single-particle mass spectrometry of tropospheric aerosol particles, *J. Geophys. Res. Atmos.*, 111, <https://doi.org/10.1029/2006JD007340>, 2006.
- 580 Murphy, S. M., Agrawal, H., Sorooshian, A., Padró, L. T., Gates, H., Hersey, S., Welch, W. A., Jung, H., Miller, J. W., Cocker, D. R. I., Nenes, A., Jonsson, H. H., Flagan, R. C., and Seinfeld, J. H.: Comprehensive Simultaneous Shipboard and Airborne Characterization of Exhaust from a Modern Container Ship at Sea, *Environ. Sci. Technol.*, 43, 4626–4640, <https://doi.org/10.1021/es802413j>, 2009.
- 585 Ndour, M., D’Anna, B., George, C., Ka, O., Balkanski, Y., Kleffmann, J., Stemmler, K., and Ammann, M.: Photoenhanced uptake of NO₂ on mineral dust: Laboratory experiments and model simulations, *Geophys. Res. Lett.*, 35, <https://doi.org/10.1029/2007GL032006>, 2008.
- Ndour, M., Conchon, P., D’Anna, B., Ka, O., and George, C.: Photochemistry of mineral dust surface as a potential atmospheric renoxification process, *Geophys. Res. Lett.*, 36, <https://doi.org/10.1029/2008GL036662>, 2009.
- 590 Passig, J., Schade, J., Irsig, R., Li, L., Li, X., Zhou, Z., Adam, T., and Zimmermann, R.: Detection of ship plumes from residual fuel operation in emission control areas using single-particle mass spectrometry, *Atmos. Meas. Tech.*, 14, 4171–4185, <https://doi.org/10.5194/amt-14-4171-2021>, 2021.
- 595 Qin, X., Chen, Z., Gong, Y., Dong, P., Cao, Z., Hu, J., and Xu, J.: Persistent Uptake of H₂O₂ onto Ambient PM_{2.5} via Dark-Fenton Chemistry, *Environ. Sci. Technol.*, 56, 9978–9987, <https://doi.org/10.1021/acs.est.2c03630>, 2022.
- Schlesinger, W. H., Klein, E. M., and Vengosh, A.: Global biogeochemical cycle of vanadium, *Proc. Natl. Acad. Sci.*, 114, E11092-E11100, <https://doi.org/10.1073/pnas.1715500114>, 2017.
- 600 Shafer, M. M., Toner, B. M., Overdier, J. T., Schauer, J. J., Fakra, S. C., Hu, S., Herner, J. D., and Ayala, A.: Chemical Speciation of Vanadium in Particulate Matter Emitted from Diesel Vehicles and Urban Atmospheric Aerosols, *Environ. Sci. Technol.*, 46, 189–195, <https://doi.org/10.1021/es200463c>, 2012.
- 605 Singh, H. B., Gregory, G. L., Anderson, B., Browell, E., Sachse, G. W., Davis, D. D., Crawford, J., Bradshaw, J. D., Talbot, R., Blake, D. R., Thornton, D., Newell, R., and Merrill, J.: Low ozone in the marine boundary layer of the tropical Pacific Ocean: Photochemical loss, chlorine atoms, and entrainment, *J. Geophys. Res. Atmos.*, 101, 1907–1917, <https://doi.org/10.1029/95JD01028>, 1996.

- 610 Song, H., Chen, X., Lu, K., Zou, Q., Tan, Z., Fuchs, H., Wiedensohler, A., Moon, D. R., Heard, D. E., Baeza-Romero, M.-T., Zheng, M., Wahner, A., Kiendler-Scharr, A., and Zhang, Y.: Influence of aerosol copper on HO₂ uptake: a novel parameterized equation, *Atmos. Chem. Phys.*, 20, 15835–15850, <https://doi.org/10.5194/acp-20-15835-2020>, 2020.
- 615 Song, S.-K., Shon, Z.-H., Moon, S.-H., Lee, T.-H., Kim, H.-S., Kang, S.-H., Park, G.-H., and Yoo, E.-C.: Impact of international Maritime Organization 2020 sulfur content regulations on port air quality at international hub port, *J. Clean Prod.*, 347, 131298, <https://doi.org/10.1016/j.jclepro.2022.131298>, 2022.
- 620 Thompson, C. R., Wofsy, S. C., Prather, M. J., Newman, P. A., Hanisco, T. F., Ryerson, T. B., Fahey, D. W., Apel, E. C., Brock, C. A., Brune, W. H., Froyd, K., Katich, J. M., Nicely, J. M., Peischl, J., Ray, E., Veres, P. R., Wang, S., Allen, H. M., Asher, E., Bian, H., Blake, D., Bourgeois, I., Budney, J., Bui, T. P., Butler, A., Campuzano-Jost, P., Chang, C., Chin, M., Commane, R., Correa, G., Crounse, J. D., Daube, B., Dibb, J. E., DiGangi, J. P., Diskin, G. S., Dollner, M., Elkins, J. W., Fiore, A. M., Flynn, C. M., Guo, H., Hall, S. R., Hannun, R. A., Hills, A., Hints, E. J., Hodzic, A., Hornbrook, R. S., Huey, L. G., Jimenez, J. L., Keeling, R. F., Kim, M. J., Kupc, A., Lacey, F., Lait, L. R., Lamarque, J.-F., Liu, J., McKain, K., Meinardi, S., Miller, D. O., Montzka, S. A., Moore, F. L., Morgan, E. J., Murphy, D. M., Murray, L. T., Nault, B. A., Neuman, J. A., Nguyen, L., Gonzalez, Y., Rollins, A., Rosenlof, K., Sargent, M., Schill, G., Schwarz, J. P., Clair, J. M. S., 625 Steenrod, S. D., Stephens, B. B., Strahan, S. E., Strode, S. A., Sweeney, C., Thames, A. B., Ullmann, K., Wagner, N., Weber, R., Weinzierl, B., Wennberg, P. O., Williamson, C. J., Wolfe, G. M., and Zeng, L.: The NASA Atmospheric Tomography (ATom) Mission: Imaging the Chemistry of the Global Atmosphere, *Bull. Am. Meteorol. Soc.*, 103, E761–E790, <https://doi.org/10.1175/BAMS-D-20-0315.1>, 2022.
- 630 Thomson, D. S., Middlebrook, A. M., and Murphy, D. M.: Thresholds for Laser-Induced Ion Formation from Aerosols in a Vacuum Using Ultraviolet and Vacuum-Ultraviolet Laser Wavelengths, *Aerosol Sci. Technol.*, 26, 544–559, <https://doi.org/10.1080/02786829708965452>, 1997.
- 635 Tsamalis, C., Chédin, A., Pelon, J., and Capelle, V.: The seasonal vertical distribution of the Saharan Air Layer and its modulation by the wind, *Atmospheric Chem. Phys.*, 13, 11235–11257, <https://doi.org/10.5194/acp-13-11235-2013>, 2013.
- 640 Uhler, A. D., Stout, S. A., Douglas, G. S., Healey, E. M., and Emsbo-Mattingly, S. D.: 13 - Chemical character of marine heavy fuel oils and lubricants, in: *Standard Handbook Oil Spill Environmental Forensics (Second Edition)*, edited by: Stout, S. A. and Wang, Z., Academic Press, Boston, 641–683, <https://doi.org/10.1016/B978-0-12-803832-1.00013-1>, 2016.
- 645 UNCTAD: United Nations Conference on Trade and Development (UNCTAD), 'Review of Maritime Transport 2018', 2018.
- UNCTAD: United Nations Conference on Trade and Development (UNCTAD), 'Review of Maritime Transport 2022', 2022.
- 650 Underwood, G. M., Miller, T. M., and Grassian, V. H.: Transmission FT-IR and Knudsen Cell Study of the Heterogeneous Reactivity of Gaseous Nitrogen Dioxide on Mineral Oxide Particles, *J. Phys. Chem. A*, 103, 6184–6190, <https://doi.org/10.1021/jp991586i>, 1999.
- Viana, M., Amato, F., Alastuey, A., Querol, X., Moreno, T., García Dos Santos, S., Hecce, M. D., and Fernández-Patier, R.: Chemical Tracers of Particulate Emissions from Commercial Shipping, *Environ. Sci. Technol.*, 43, 7472–7477, <https://doi.org/10.1021/es901558t>, 2009.

- 655 Wang, X., Shen, Y., Lin, Y., Pan, J., Zhang, Y., Louie, P. K. K., Li, M., and Fu, Q.: Atmospheric pollution from ships and its impact on local air quality at a port site in Shanghai, *Atmos. Chem. Phys.*, 19, 6315–6330, <https://doi.org/10.5194/acp-19-6315-2019>, 2019.
- 660 Wu, D., Li, Q., Ding, X., Sun, J., Li, D., Fu, H., Teich, M., Ye, X., and Chen, J.: Primary Particulate Matter Emitted from Heavy Fuel and Diesel Oil Combustion in a Typical Container Ship: Characteristics and Toxicity, *Environ. Sci. Technol.*, 52, 12943–12951, <https://doi.org/10.1021/acs.est.8b04471>, 2018.
- 665 Wu, L., Xu, Y., Wang, Q., Wang, F., and Xu, Z.: Mapping Global Shipping Density from AIS Data, *J. Navig.*, 70, 67–81, <https://doi.org/10.1017/S0373463316000345>, 2017.
- Xiong, X., Wang, Z., Cheng, C., Li, M., Yun, L., Liu, S., Mao, L., and Zhou, Z.: Long-Term Observation of Mixing States and Sources of Vanadium-Containing Single Particles from 2020 to 2021 in Guangzhou, China, *Toxics*, 11, 339, <https://doi.org/10.3390/toxics11040339>, 2023.
- 670 Ye, D., Klein, M., Mulholland, J. A., Russell, A. G., Weber, R., Edgerton, E. S., Chang, H. H., Sarnat, J. A., Tolbert, P. E., and Ebel, S. S.: Estimating Acute Cardiovascular Effects of Ambient PM_{2.5} Metals, *Environ. Health Perspect.*, 126(027007), 1–10, <https://doi.org/10.1289/EHP2182>, 2018.
- 675 Yu, G., Zhang, Y., Yang, F., He, B., Zhang, C., Zou, Z., Yang, X., Li, N., and Chen, J.: Dynamic Ni/V Ratio in the Ship-Emitted Particles Driven by Multiphase Fuel Oil Regulations in Coastal China, *Environ. Sci. Technol.*, 55, 15031–15039, <https://doi.org/10.1021/acs.est.1c02612>, 2021.
- 680 Yuan, T., Song, H., Wood, R., Wang, C., Oreopoulos, L., Platnick, S. E., von Hippel, S., Meyer, K., Light, S., and Wilcox, E.: Global reduction in ship-tracks from sulfur regulations for shipping fuel, *Sci. Adv.*, 8, eabn7988, <https://doi.org/10.1126/sciadv.abn7988>, 2022.
- Zhang, F., Chen, Y., Tian, C., Wang, X., Huang, G., Fang, Y., and Zong, Z.: Identification and quantification of shipping emissions in Bohai Rim, China, *Sci. Total Environ.*, 497–498, 570–577, <https://doi.org/10.1016/j.scitotenv.2014.08.016>, 2014.
- 685 Zhou, S., Zhou, J., and Zhu, Y.: Chemical composition and size distribution of particulate matters from marine diesel engines with different fuel oils, *Fuel*, 235, 972–983, <https://doi.org/10.1016/j.fuel.2018.08.080>, 2019.
- 690 Zhou, Y., Wang, Z., Pei, C., Li, L., Wu, M., Wu, M., Huang, B., Cheng, C., Li, M., Wang, X., and Zhou, Z.: Source-oriented characterization of single particles from in-port ship emissions in Guangzhou, China, *Sci. Total Environ.*, 724, 138179, <https://doi.org/10.1016/j.scitotenv.2020.138179>, 2020.